Senolytics alleviate cyclophosphamide-induced premature ovarian insufficiency by eliminating senescent cells

Huina Su,* Ruiqiong Ma,* Dehui Su,* Cheng Tan, Ye Zhu, Xin Yang

Department of Obstetrics and Gynecology, Peking University People's Hospital, Beijing, China

*These authors contributed equally to this work and share first authorship

ABSTRACT

Alkylating agents, particularly cyclophosphamide (CY), are known for their high toxicity, which can lead to iatrogenic premature ovarian insufficiency (POI) and infertility in young cancer survivors. Currently, effective prevention and treatment strategies remain limited. Given that chemotherapy induces cellular senescence, we investigated the therapeutic potential of dasatinib (D) and quercetin (Q), a senolytic combination known to eliminate senescent cells. Using a CY-induced murine model of ovarian injury, we found that CY treatment increased the accumulation of senescent cells in the ovaries. The resulting senescence-associated secretory phenotype (SASP) led to a deterioration of the ovarian microenvironment, characterized by increased follicular atresia and a decline in follicle quantity, ultimately culminating in POI. Our findings demonstrate that DQ therapy effectively mitigated CY-induced damage by clearing senescent cells and reducing SASP secretion. Clinically, DQ administration restored sex hormone levels and regularity of the estrous cycle, resulting in an overall increase in follicle numbers across all developmental stages. Furthermore, DQ treatment significantly normalized estrous cyclicity, restoring regular cycles in 60% of the CY+DQ mice compared to only ~15% in the CY-alone group ($p<0.0001$). RNA sequencing analysis revealed that DQ treatment upregulated Pagr1a, a gene associated with extraembryonic development, while downregulating genes involved in senescence induction (*Itgb3, Wnt10b, Vegfa*) and immune function (*A2m, Ccl21d*). These results suggest that senescent cells drive CY-induced ovarian damage and that DQ represents a promising therapeutic strategy for preserving the ovarian reserve and endocrine function in female cancer patients.

Key words: premature ovarian insufficiency; cell senescence; dasatinib; quercetin; cyclophosphamide.

Correspondence: Xin Yang, Department of Obstetrics and Gynecology, Peking University People's Hospital, 11th Xizhimen South Street, Xicheng District, Beijing 100044, China. E-mail: xinyang1965@163.com.
Ye Zhu, Department of Obstetrics and Gynecology, Peking University People's Hospital, 11th Xizhimen South Street, Xicheng District, Beijing 100044, China. E-mail: zhuye@pku.edu.cn

Contributions: Huina Su, Xin Yang, study designing, data interpretation. Huina Su, Ruiqiong Ma, Dehui Su, Cheng Tan, Ye Zhu, experiments and analysis performing. Huina Su, Ruiqiong Ma, analysis and interpretation of data. Huina Su, writing - original draft. All authors made a substantive intellectual contribution, read and approved the final version of the manuscript, agreed to be accountable for all aspects of the work.

Conflict of interest: the authors declare no competing interests.

Ethics approval: this study was approved by the Experimental Animal Ethics Committee at Peking University People's Hospital (PU-AE-24021).

Funding: this study was supported by the National Natural Science Foundation of China (Grant no. 82402289).

Data availability statement: the data that support the findings of this study are available from the corresponding author upon reasonable request.

Introduction

The term adolescents and young adults (AYA) refers to individuals who have been diagnosed with cancer between the ages of 15 and 39. This specific group of individuals has unique medical and supportive care needs.[1] The global occurrence of cancer in AYAs is on the rise, with a documented frequency of 52.3 cases per 100, 000 individuals each year in 2019.[2] Lately, there has been an encouraging trend in the survival rates of AYA battling cancer, as statistics indicate that approximately 85% of these patients have a five-year survival rate in developed nations.[3] The emergence of these patterns has resulted in a growing number of cancer survivors within the reproductive age groups. Nevertheless, a significant number of young individuals who have overcome cancer may encounter enduring consequences resulting from their therapy, such as premature ovarian insufficiency (POI) and infertility. Additionally, there are long-term complications like cognitive decline and cardiovascular risks associated with menopause. Many chemotherapy drugs employed in cancer treatment have detrimental effects on ovarian function, consequently elevating the likelihood of POI.[4] Cyclophosphamide (CY), a widely employed initial treatment for diverse types of cancer and autoimmune conditions, is notorious for its detrimental effects on the ovaries and has been linked to amenorrhea and POI.[5]

It is well established that chemotherapy has the capacity to induce cell senescence and apoptosis. Research has demonstrated that the ovary's actively dividing cells are more vulnerable to the toxic effects of chemotherapy compared to those in a dormant state.[6] Furthermore, studies have shown that chemotherapeutic agents, such as CY, induce structural and endocrine impairments in ovarian follicles and granulosa cells, ultimately disrupting fertility.[7] Even though embryo, oocyte, and ovarian tissue freezing are the primary methods for preserving fertility in women diagnosed with cancer, The widespread use of these items is hindered by safety and ethical concerns. Therefore, investigating the pathogenesis of CY-induced POI and pursuing safer and more effective treatments to enhance ovarian function in POI patients will greatly influence the field of reproductive endocrinology.[8,9]

Cellular senescence refers to a lasting and stable cessation of cell division caused by diverse types of cellular stress. Senescent cells are characterized by the increased expression of p16 and p21, along with structural and metabolic changes, as well as constant activation of DNA damage signaling pathways. This is characterized by an increased secretory state, known as the senescence-associated secretory phenotype (SASP). The SASP comprises pro-inflammatory cytokines, chemokines, growth factors, and enzymes, which collectively play a role in organ senescence, age-related diseases, and chronic illnesses. Recent studies indicate that granulosa cells experiencing senescence and an aberrant inflammatory condition are significant contributors to the development of POI.[10] Research has demonstrated that CY induces senescence in granulosa cells, resulting in aberrant follicular morphology and hormonal dysregulation, which collectively compromise fertility.[7] It is well-established that cellular senescence is a fundamental driver of age-related pathologies; consequently, therapeutic strategies targeting senescent cells represent a promising avenue for clinical intervention.

Granulosa cells (GCs) are highly proliferative and particularly vulnerable to CY-induced toxicity. CY causes severe DNA damage in GCs, rapidly driving them into cellular senescence rather than apoptosis.[11] These accumulating senescent GCs exhibit a robust SASP -releasing pro-inflammatory factors like IL-6 and IL-8- that severely deteriorates the ovarian microenvironment. By disrupting somatic-germ cell communication and triggering follicular atresia and fibrosis, this GC-driven SASP acts as a primary driver of chemotherapy-induced POI.[12] Given that these lingering senescent GCs continuously drive follicular damage, selectively removing them offers a direct and promising approach to rescue the ovarian microenvironment. Dasatinib (D) and quercetin (Q) together form a renowned senolytic therapy that efficiently removes senescent cells. Numerous studies have shown that it is effective in prolonging healthy lifespans and improving age-related diseases.[13] However, the processes through which cyclophosphamide causes ovarian damage and the possible involvement of senolytics in reducing cyclophosphamide-induced ovarian injury are still uncertain. During our study, we created a cyclophosphamide-induced ovarian injury model and found that giving mice cyclophosphamide resulted in an increase in senescent cells in their ovarian tissue. The accumulation of senescent cells led to the release of SASP components, which intensified the ovarian microenvironment and played a role in POI. Our findings suggest that the combined administration of D and Q attenuates cyclophosphamide-triggered ovarian toxicity by clearing senescent cells and suppressing the senescence-associated secretory phenotype (SASP), highlighting cellular senescence as a pivotal mechanism in chemotherapy-induced ovarian injury. The DQ regimen could potentially serve as an effective strategy to protect fertility in female cancer patients during their treatment.

Materials and Methods

Animal care and drug administration

Forty sexually mature female C57BL/6 mice, aged six weeks, were procured from Beijing Weitong Lihua Experimental Animal Technology Co., Ltd. (Beijing, China) These mice were individually housed under a 12-hlight/dark cycle for one week to acclimatize before being randomly assigned to four groups: Control (CTR), CY, CY+DQ, and DQ. The experimental design is depicted in Figure 1A. Cyclophosphamide (CY; Catalog No. C0768) was purchased from Sigma-Aldrich (Taufkirchen, Germany) and stored at 4°C protected from light. The senolytic agents, dasatinib (Catalog No. D-3307; LC Laboratories, Woburn, MA, USA) and quercetin (Catalog No. Q4951; Sigma-Aldrich), were prepared according to the manufacturers' instructions, aliquoted, and strictly stored at -20°C to maintain stability. For *in vivo* experiments, dasatinib (5 mg/kg) and quercetin (50 mg/kg) were dissolved in polyethylene glycol (Catalog No. 25322-68-3; Shanghai Macklin Biochemical Co., Ltd., Shanghai, China). Mice in the CY+DQ and DQ groups were administered this senolytic cocktail intragastrically twice weekly for four weeks, while the Control and CY groups received an equivalent volume of vehicle (10% polyethylene glycol). One week after the initiation of senotherapy, the CY and CY+DQ groups received a single intraperitoneal (i.p.) injection of CY (75 mg/kg in 0.1 mL). Concurrently, the Control and DQ groups received an equivalent i.p. injection of 0.1 mL PBS (Catalog No. G4202; Servicebio Technology Co., Ltd., Wuhan, China). The specific dosages and administration protocols were strategically selected to balance POI induction with the systemic safety window. A single intraperitoneal dose of CY (75 mg/kg) was utilized because it reliably induces acute follicular depletion and mirrors the clinical endocrine profile of POI without causing unmanageable systemic toxicity or mortality. For the senolytic intervention, an intermittent dosing strategy (twice weekly) was employed. This 'hit-and-run' pharmacological approach efficiently

clears accumulating senescent cells while minimizing potential off-target toxicities associated with continuous Dasatinib exposure. The four-week treatment duration was explicitly chosen to encompass multiple murine estrous cycles, ensuring sufficient time to accurately evaluate the long-term structural and functional recovery of the ovaries.[14] Four weeks following the initial dosage, the mice were sacrificed, and samples of blood, ovary, and oviduct were collected.

Cell culture and treatment

KGN cells (BNCC337610) from the Beijing Beina Chuanglian Biotechnology Research Institute (Beijing, China) were cultivated in a culture medium consisting of DMEM/F-12 (C11330500BT; Gibco, Rockville, MD, USA) supplemented with 10% fetal bovine serum (FBS) (10099-141C; Gibco) and antibiotics (GA2312026, Servicebio), in a humidified atmosphere at 37°C with 5% CO_2. In a laboratory setting, cultured KGN cells were subjected to phosphoramide mustard (PM), a metabolite of CY, for treatment purposes. To evaluate its capability to trigger senescence in granulosa cells. In the PM+DQ and DQ groups, after KGN cells attached to the medium, Dasatinib (1 nmol/L) and Quercetin (20 μmol/L) were incorporated. After a span of 48 hours, the medium utilized by all groups was substituted. The Control and DQ groups remained in DMEM/F-12 growth medium for an extra 48 h. The remaining two groups received PM treatment (10159-53-2, Apexbio, USA, 30 μmol/L) for an additional 48 h.

CCK-8 assay

The CCK-8 assay (product no. 40203ES80; Yeasen Biotechnology Co., Ltd., Shanghai, China) was employed to assess cell viability following the manufacturer's guidelines. KGN cells were seeded onto 96-well plates at a density of 2, 000 cells per well and then placed in complete medium for a period of 24 h to culture them. After undergoing the specified treatments, a total of 100 μL of DMEM was added to each well, which contained 10 μL of CCK-8 solution. The cells were then incubated for a duration of 2 h. A microplate reader was employed to measure absorbance at 450 nm, following which the proliferation curve was calculated.

Senescence-associated (SA-) β-gal staining

Following the manufacturer's guidelines (C0602), SA-β-gal staining was performed on KGN cells and frozen ovarian sections (Beyotime Biotechnology, Shanghai, China). KGN cells underwent a pre-treatment process involving washing, fixing, and staining, whereas frozen ovarian slices were thawed before staining.

RT-qPCR analysis

Total RNA was extracted using TRIzol reagent (R1100; Solarbio) and subsequently quantified and evaluated for purity. The RNA was then converted into complementary DNA (cDNA) through reverse transcription, employing the Hifair III 1st Strand cDNA Synthesis SuperMix for qPCR (11141ES60; Yeasen). Quantitative PCR (qPCR) was carried out using Hieff qPCR SYBR Green Master Mix (11201ES08; Yeasen) on the BIO-RAD real-time PCR system. To ensure accuracy, each reaction was performed three times, and GAPDH served as an internal reference. Table 1 provides detailed information about primer sequences; the relative gene expression was determined through the $2^{-\Delta\Delta Ct}$ method.

Analysis of mitochondrial membrane potential

The JC-1 assay kit (C2006; Beyotime, Shanghai, China) was employed to measure mitochondrial membrane potential (MMP), adhering to the manufacturer's guidelines. In summary, the cells underwent a rinsing process using PBS and were subsequently provided with fresh medium to ensure their continued viability. Afterwards, they underwent treatment with an identical quantity of JC-1 staining solution for a duration of 20 minat a temperature of 37°C. Fluorescence images were obtained through the use of a Leica K5 (Germany) microscope, and the ratio of red to green fluorescence intensity was subsequently analyzed using ImageJ software.

Cell apoptosis detection using TUNEL

Before staining, ovarian sections underwent dewaxing and hydration processes as per the instructions provided in the manual for the Colorimetric TUNEL Apoptosis Assay Kit (G1507; Servicebio) conducted an evaluation of apoptosis using the One Step TUNEL Apoptosis Kit (C1089; Beyotime) following the manufacturer's guidelines. To quantify the results, the counts of TUNEL-positive and total granulosa cells in antral follicles were measured with ImageJ software. To recap, the KGN cells that were attached went through a sequence of procedures, such as cleansing, fixing, and making them permeable. Following equilibration, TUNEL labeling is performed using a reaction mixture containing

Table 1. Primer sequences.

Genes	Species	Forward primer (5'-3')	Reverse primer (5'-3')
GAPDH	Mouse	ACCACAGTCCATGCCATCAC	TCCACCACCCTGTTGCTGTA
Ki-67	Mouse	ATCATTGACCGCTCCTTTAGGT	GCTCGCCTTGATGGTTCCT
IL-6	Mouse	CAGAGGATACCACTCCCAAC	CAATCAGAATTGCCATTGCAC
MMP3	Mouse	CCTGATGT-TGGTGGCTTCA	TCCTGTAGGTGATGTGGGATTTC
P16	Mouse	CCCAACGCCCCGAACT	GCAGAAGAGCTGCTACGTGAA
P21	Mouse	GCAGATCCACAGCGATATCC	CAACTGCTCACTGTCCACGG
P53	Mouse	AGAGACCGCCGTACAGAAGA	CTGTAGCATGGGCATCCTTT
Ki67	Human	AGAAGAAGTGGTGCTTCGGAA	AGTTTGCGTGGCCTGTACTAA
γ-H2AX	Human	GGCCTCCCAGGAGTACTAAGA	CTCTTTCCATGAGGGCGGTG
P53	Human	CCTCAGCATCTTATCCGAGTGG	GG ATG GTG GTACAGTCAGAGC
IL-6	Human	CGGCTACATCTTTGGAATCTTC	GCCCAGCTATGAACTCCTTC
IL-8	Human	AGGACAAGAGCCAGGAAGAA	GGGTGGAAAGGTTTGGAGTATG
CCL-2	Human	CATCTCCTACACCCCACGAAG	GGGTTGGCACAGAAACGTC
GAPDH	Human	GGAAGGGCTCATGACCACAG	ACAGTCTTCTGGGTGGCAGTG

TdT enzyme and labeled nucleotides, after which incubation takes place. Following the mounting process, the samples underwent examination *via* fluorescence microscopy to detect TUNEL-positive nuclei, a characteristic feature of apoptotic cells.

Serum hormone measurement

The levels of anti-Müllerian hormone (AMH), follicle-stimulating hormone (FSH), and estradiol (E2) in serum were quantified utilizing commercial ELISA kits from Elabscience Biotechnology Co., Ltd. (Wuhan, China). All assays (E-EL-M3015, E-EL-M0511c, and E-OSEL-M0002, respectively) were performed in strict accordance with the manufacturer's guidelines.

Estrous cycle monitoring

For a continuous five-week span, mice had vaginal smears collected from them every day between roughly 9 and 11 in the morning. In order to acquire vaginal cells, it is necessary to undergo a specific procedure. A sterile cotton swab was meticulously inserted into the vaginal cavity of the mice and then carefully withdrawn to gather cells and secretions onto pristine glass slides. Through microscopic examination of stained slides, it becomes possible to distinguish various cell type characteristics of each phase of the estrous cycle, such as proestrus, estrus, metestrus, and diestrus. Mice displaying consistent cycling behavior, progressing sequentially through proestrus, estrus, metestrus, and diestrus within a 4- to 6-day span, were classified as having regular cycles. Cycles were categorized as 'irregular' if they met specific threshold criteria, including a prolonged diestrus phase lasting for 3 or more consecutive days, a total cycle length extending beyond 6 days, or the absence of detectable cyclical progression.[15,16]

Follicle counting

The ovaries were preserved using 4% paraformaldehyde, embedded in paraffin, and subsequently cut into 5 µm sections. Every fifth slide underwent staining with hematoxylin and eosin (H&E) and subsequent examination under a light microscope by two individuals who were blinded to the section groups. Following the guidelines outlined in established protocols.[17]

Immunohistochemistry staining

Ovarian sections underwent immunostaining with the use of various antibodies, such as the anti-CDKN2A/p16INK4A mouse monoclonal antibody (ab267833, 1:500; Abcam, Cambridge, MA, USA) and p21 (28248-1-AP, 1:300; Proteintech, Rosemont, IL, USA), p53 (sc-126, 1:150; Santa Cruz Biotechnology, Santa Cruz, CA, USA), and recombinant anti-gamma H2A. X (phospho S139) antibody (ab81299, 1:400, Abcam, Cambridge, MA, USA), recombinant anti-Ki67 antibody (ab16667, 1:400; Abcam), rabbit anti-8-OHdG/DNA/RNA damage antibody (bs-1278R, The following rephrased sentence maintains the original meaning but with substantial alterations and increases in length while ensuring seamless connectivity between the words in short sentences: HO1 (66743-1-Ig, 1:1000; Proteintec), SOD2 (bs-20667R, 1:300; Bioss, Wuhan, China), and another Bioss product from China at a concentration of 1:300 were utilized. The immunohistochemical analysis was conducted multiple times, specifically at least three instances, using the identical set of samples.

Sirius Red staining

Ovarian sections are processed by removing paraffin and rehydrating them before staining with Sirius Red solution (BP-DL029; Sbjbio, Beijing, China). After the staining process, the sections were subjected to washing and dehydration procedures before being covered with neutral balsam to enable subsequent imaging and analysis.

Statistical analysis

All statistical analyses were performed using GraphPad Prism version 10.0 (GraphPad Software, Boston, MA, USA). Quantitative data are presented as the mean ± SD. For in vitro immunofluorescence quantification (*e.g.*, JC-1 and TUNEL assays), the sample size (n) denotes the number of independent microscopic fields of view randomly captured and analyzed across at least three independent biological replicates. Before statistical comparisons, the normal distribution of the data was verified using the Shapiro-Wilk test, and the homogeneity of variances was assessed using the Brown-Forsythe test. For multi-group comparisons, a one-way analysis of variance (ANOVA) was conducted, followed by Tukey's *post-hoc* test for multiple comparisons. A *p*-value of <0.05 was considered statistically significant.

Results

Effects of DQ therapy on body mass, ovarian function, and estrous cycle in CY-induced POI mice

A POI mouse model was induced using CY to investigate the therapeutic potential of DQ. Subsequently, the mice received intragastric administration of the DQ solution over four weeks. Figure 1A depicts the experimental setup, providing a visual representation of its organization. In order to evaluate the degree of ovarian impairment and the protective function of DQ thoroughly, we conducted a thorough analysis of the mice's body weight both prior to and following the experiment. In the experiment, it was observed that CY had a significant effect on reducing the body weight of the mice. However, the reduction was reversed by DQ therapy (Figure 1B). Furthermore, at the conclusion of the experiment, the ovaries' weight was measured and subsequently used to calculate the ovarian index, which is defined as the ratio of ovarian weight to body weight. Our research revealed that DQ had a substantial impact on elevating the ovarian index, which was subsequently diminished as a result of POI (Figure 1C). To evaluate the impact of CY and DQ treatment on ovarian function in mice, we analyzed the concentrations of reproductive hormones in their serum. Compared to the CTR, POI mice exhibited a significant decrease in mean serum E2 levels ($p<0.05$) and AMH ($p<0.05$), alongside a significant rise in average serum FSH levels ($p<0.01$) as depicted in Figure 1D. The wider variance observed in the FSH levels of the CY group reflects the expected biological heterogeneity in the physiological response to chemotherapy, as individual mice experience varying degrees of acute follicular depletion and subsequent endocrine disruption. As shown in Figure 1D, treatment with DQ resulted in a substantial impact on serum hormone levels when compared to the CY group. In particular, the average concentrations of AMH ($p<0.01$) and E2 ($p<0.05$) exhibited an increase. There was a significant decline in the average serum level of FSH, as indicated by the *p*-value of less than 0. 01 (Figure 1D). To sum up, after administering DQ, the abnormal levels of serum hormones showed a gradual improvement. Irregular estrous cycles may suggest possible problems with steroid production and impaired ovarian function.[18] To evaluate the degree of ovarian damage and the protective impact of DQ, we monitored estrous cyclicity *via* vaginal smear analysis. As depicted in Figure 1A, CTR mice displayed consistent estrous cycles spanning 4-5 days, progressing normally through proestrus, estrus, metestrus, and diestrus phases in sequence. In con-

trast, CY-treated mice exhibited severe cycle disruptions, primarily characterized by prolonged diestrus and overall irregularity. However, senolytic intervention effectively rescued this phenotype; the rate of regular estrous cycles was significantly restored in the CY+DQ group (60%) compared to the CY-alone group (~15%) (p<0.0001, Figure 1E). These quantitative improvements demonstrate that DQ therapy successfully mitigates CY-induced damage and restores systemic reproductive cyclicity in POI mice.

DQ mitigates ovarian follicle damage and SASP expression in CY-induced POI mice

After performing H&E staining, we analyzed the structural alterations in ovarian tissue. Analysis of the tissues from both the CTR and DQ groups showed that they had normal morphology with a plentiful presence of follicles at different developmental stages (Figure 2A). On the other hand, CY therapy led to ovarian atrophy, as shown by a decrease in follicle numbers at all stages and the occurrence of stromal fibrosis. In contrast, the CY+DQ group exhibited significant enhancement, indicating preservation of various primordial, primary, secondary, and antral follicles, along with a lower number of atretic follicles (Figure 2B). Therefore, the application of DQ therapy successfully mitigated the detrimental effects of CY exposure on ovarian follicles. To determine if DQ had an impact on the accumulation of senescent cells in ovaries damaged by cyclophosphamide, we assessed SASP factor expression across all groups using q-PCR analysis. In comparison to the CY group, DQ had a downregulating effect on the mRNA levels of *Ki-67* (p<0.05). The expression levels of *p16*

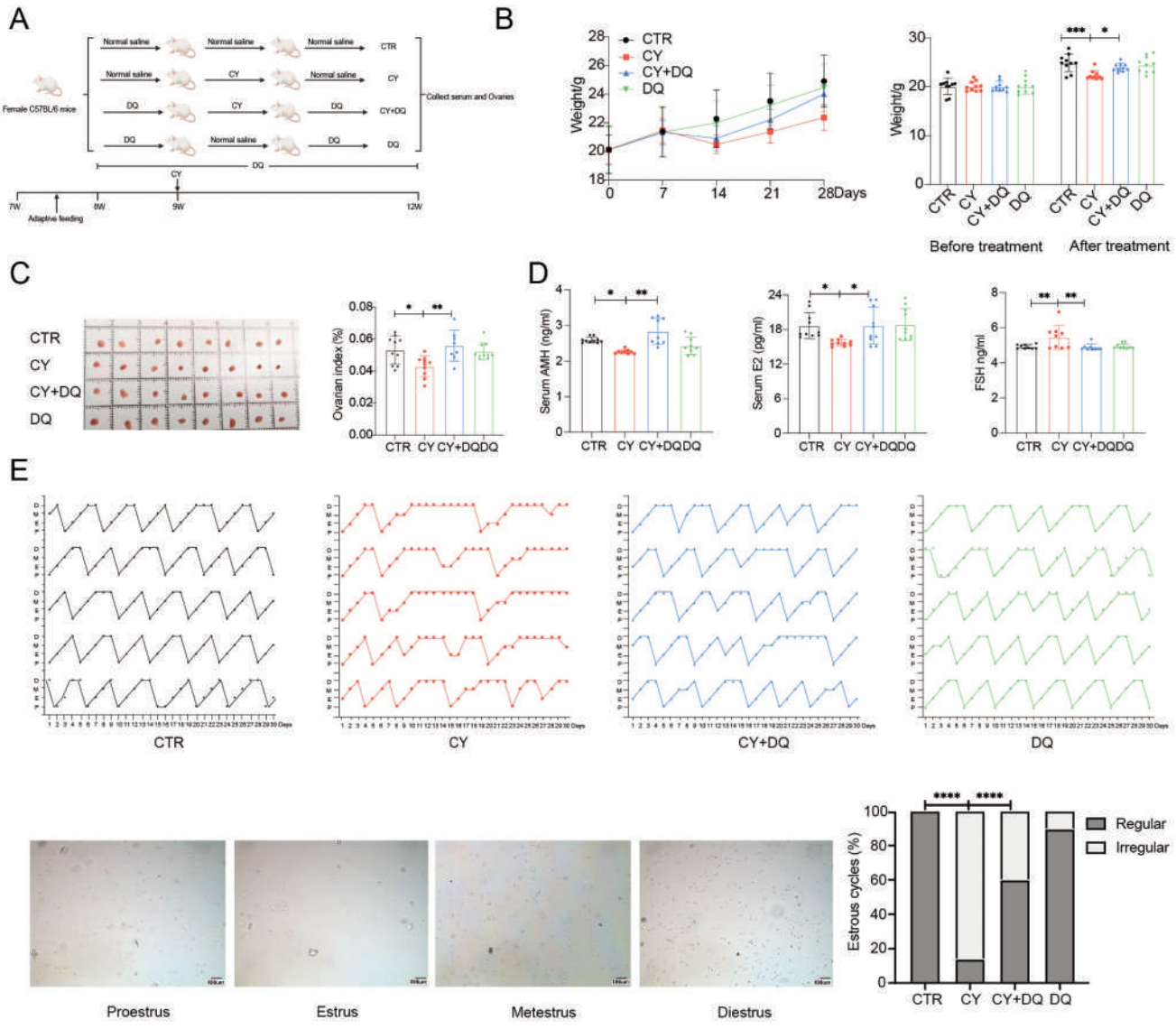

Figure 1. DQ treatment improved body weight, ovarian index, sex hormone levels, and the estrous cycle in POI mice. **A**) Flowchart of drug administration animal experiment; **B**) Body weight before and after the experiment (n=10). **C**) Appearance of representative ovaries and ovarian index (n=10). **D**) Serum levels of AMH, E2, and FSH (n=10). **E**) Representative estrous cycle for each mouse (n=5 for each group); cytological assessment of vaginal smears during each phase of the estrous cycle, and regular and irregular estrous cycle percentage of different medication groups (n=5); P, proestrus; E, estrus; M, metestrus; D, diestrus, scale bars: 100 μm. All values were displayed as mean ± SD. One-way ANOVA was used for statistical analysis; *p<0.05, **p<0.01, ***p<0.001; ****p<0.0001.

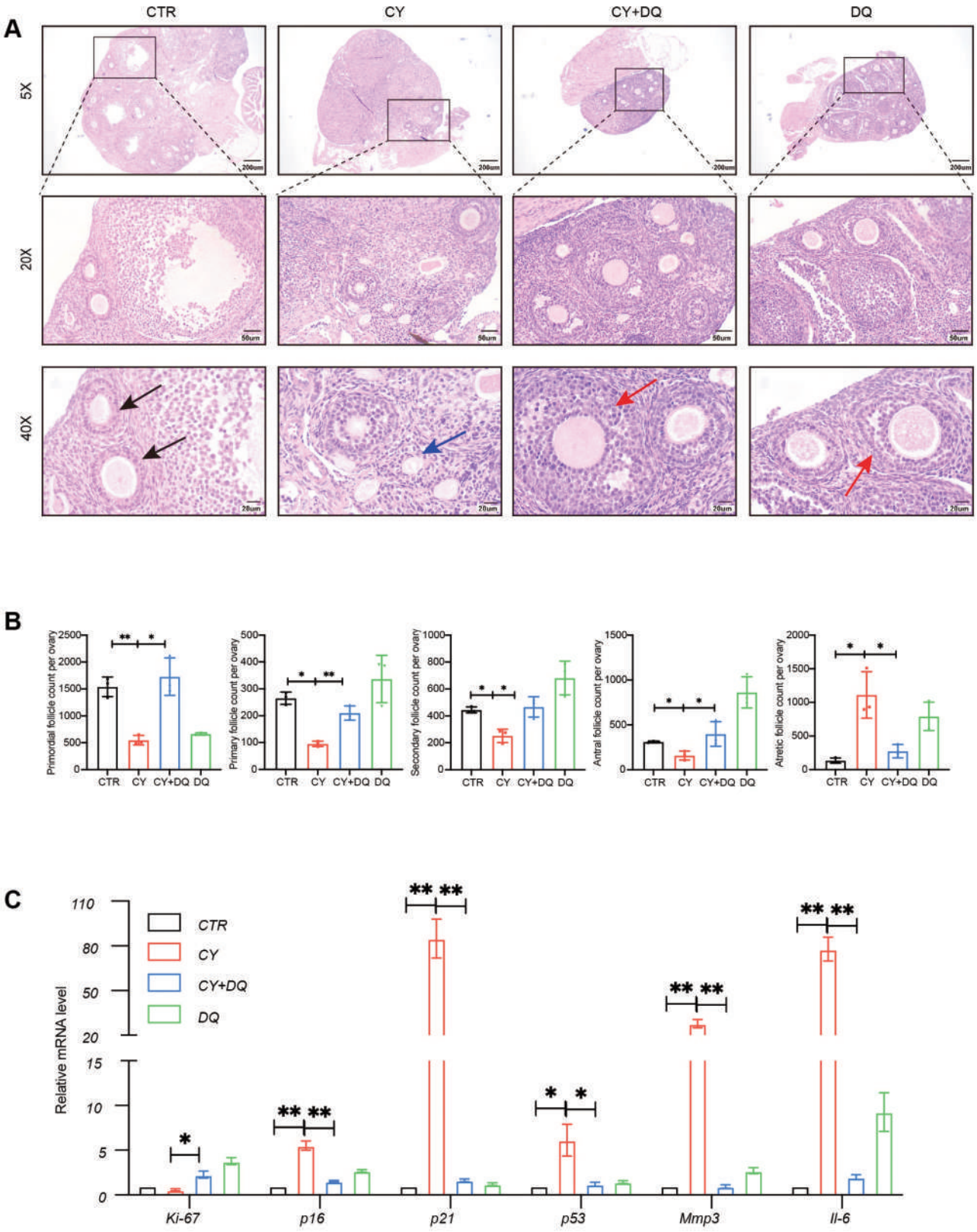

Figure 2. DQ improves the histomorphology of ovarian follicles in POI mice and attenuates the expression of SASP in CY-induced POI model mice. **A**) Representative photography by Hematoxylin & Eosin (5X, 20X, and 40X); the black, red, and blue arrows indicate secondary follicles, antral follicles, and atretic follicles, respectively; scale bars: 5X images) 200 μ; 20X images) 50 μm; 40X images) 20 μm. **B**) The number of follicles in different stages (n=3). **C**) Relative mRNA expression levels of genes related to cellular senescence in ovaries (n=3). All values were displayed as mean ± SD. One-way ANOVA was used for statistical analysis; *p<0.05, **p<0.01.

(p<0.01), *p21* (p<0.01), *p53* (p<0.05), *Mmp3* (p<0.01), and *Il-6* (p<0.01) were significantly altered, as demonstrated in Figure 2C. The results demonstrate that administering DQ successfully counteracted the effects of CY on ovarian senescence.

DQ reduces senescence, DNA damage, fibrosis, and apoptosis in CY-induced POI mice

In order to gain a clearer understanding of whether DQ therapy has the potential to alleviate senescence-induced stress in living organisms, we examined the manifestation of proliferation and senescence indicators, such as Ki-67, γ-H2AX, p16, p21, and p53, along with SA-β-gal staining in every group (Figure 3A). In comparison to the CTR group, the DQ intervention effectively decreased the heightened levels of γ-H2AX (p<0.0001). The granulosa cells of antral follicles (Figure 3A) exhibited significant differences in p21 (p<0.001), p53 (p<0.05), and p16 (p<0.001). In the ovaries treated with CY, Ki-67 staining was almost non-existent, but after undergoing DQ treatment, there was a remarkable recovery of positive Ki-67 staining, as shown in Figure 3A. Similarly, the ovaries of the CY group exhibited a rise in SA-β-gal–positive staining (p<0.0001). Following the DQ intervention, the extent of SA-β-gal–positive staining in the ovaries demonstrated a decline (p<0.0001, Figure 3A). Numerous studies have demonstrated that ongoing DNA damage and oxidative stress play a crucial role in inducing cellular senescence.[19,20] To assess the DNA damage caused by CY and the protective impact of DQ on ovarian tissue, researchers conducted 8-OHdG staining. The CY group showed a notably higher level of positive staining for 8-OHdG (p<0.0001, Figure 3B). The IHC findings further indicated a significant decrease in antioxidant markers SOD2 and HO-1 within the ovaries following exposure to CY. There is evidence of substantial oxidative DNA damage in the tissue, as shown in Figure 3B. These indices were mitigated to varying degrees in ovaries treated with CY+DQ.

The prolonged viability of senescent cells is facilitated by the activation of specific anti-apoptotic signaling pathways.[21] Prior studies have established that DQ functions as a potent senolytic agent, selectively eliminating senescent cells in both cell cultures and animal models. This clearance translates into broad physiological benefits in mice, including ameliorated cardiovascular health, superior exercise capacity, and the mitigation of age-related conditions such as osteoporosis and frailty, ultimately prolonging healthspan.[21,22] In order to evaluate the influence of senolytics on aged ovarian cells and to assess cell apoptosis and proliferation in ovaries exposed to various treatments, we carried out TUNEL staining on ovarian sections. CY triggered apoptosis in ovarian granulosa cells, whereas DQ administration resulted in elevated TUNEL staining (Figure 3B). The evidence points to the fact that DQ specifically induced apoptosis in senescent cells.

To evaluate DQ's protection against CY-induced structural damage, we assessed ovarian fibrosis. Sirius Red staining confirmed that CY significantly increased the fibrotic area, which was effectively reversed by DQ (Figure 3B). Mechanistically, senescent cells drive pathological remodeling by secreting pro-fibrotic SASP factors that hyperactivate fibroblasts and promote excessive collagen deposition. By eliminating these senescent granulosa cells, DQ halts this localized pro-fibrotic cascade, thereby rescuing the ovarian stromal architecture.

DQ regulated cell development in the CY-induced POI model mice

To investigate the molecular mechanisms underlying DQ in CY-treated ovaries, we performed transcriptome sequencing (RNA-seq) on ovarian tissues. To investigate the biological processes and signaling pathways connected with differentially expressed genes (DEGs), researchers employed Gene Ontology (GO) and Kyoto Encyclopedia of Genes and Genomes (KEGG) enrichment analyses. The heatmap visually represents the DEGs found in the CY and CY+DQ ovaries, as depicted in Figure 4A. When compared to ovaries treated with CY, the CY+DQ group showed a substantial increase in the expression of DEGs related to sperm tail development (*Oaz3, Odf1*) and extraembryonic developmental regulation (Pagr1a). FSH-regulated genes, such as Cited1, are depicted in Figure 4A. Significantly, the senolytic DQ therapy led to a reduction in the expression of genes associated with senescence induction (*Itgb3*, *Wnt10b*, *Vegfa*, *Pappa*).[23-26] In addition to genes associated with immune and inflammatory responses, such as A2m and Ccl21d,[27,28] other factors also play a role. Furthermore, the DEGs found in CY-treated ovaries and CY+DQ groups were enriched with diverse GO terms associated with hormone response, female pregnancy, and multicellular organism processes (Figure 4B). Gene set enrichment analysis (GSEA) of differential genes indicated possible participation in pathways associated with DNA replication and mismatch repair (as shown in Figure 4C). Moreover, relative to the CY cohort, DQ intervention significantly upregulated longevity-associated signaling and enriched gene sets governing the metabolism of glycine, serine, and threonine (Figure 4D).

DQ reduced CY-induced senescent granulosa cells and the SASP

To assess the potential of CY to elicit cellular senescence, we exposed KGN cells to its bioactive metabolite, PM, under *in vitro* conditions. Figure 5A depicts the flowchart of the in vitro experiment. The CCK-8 assay was employed to assess cell viability, and the proliferation curve was subsequently obtained based on these results. The proliferation curve demonstrated a substantial decline in cell viability within the PM group, while DQ was found to promote cell proliferation (Figures 5 B,C). To assess senescent stress, we employed SA-β-gal staining as a method. In Figure 5D, there is a noticeable increase in SA-β-gal–positive staining observed in KGN cells treated with PM compared to the CTR group (p<0.05). To explore the potential of DQ in mitigating senescence stress caused by CY in a laboratory setting, we conducted qPCR analyses focusing on senescence-related markers. Quantitative qPCR analysis showed a significant increase in the expression of the senescence marker *p53* (p<0.01), *γ-H2AX*, *CCL2* (p<0.01), *IL-6* (p<0.01), *IL-8* (p<0.01), and downregulation of the proliferation marker *KI-67* (p<0.01) was observed in PM-treated KGN cells, as shown in Figure 5E. Additionally, we investigated the impact of DQ on the aging process of KGN cells treated with PM. The KGN cells underwent a pretreatment process involving DQ for a duration of 48 h, followed by an incubation phase with PM lasting another 48 h. The effects of PM on cellular senescence were effectively reversed by DQ, as shown in Figure 5. Therefore, our laboratory experiments indicate that senolytic medications could potentially suppress granulosa cell aging in individuals suffering from POI.

DQ regulated cellular MMP and apoptosis in PM-induced KGN cells

To substantiate the protective efficacy of DQ against PM-mediated cytotoxicity, we evaluated mitochondrial membrane potential and apoptosis using JC-1 and TUNEL assays, respectively. The JC-1 staining demonstrated a substantial reduction in MMP levels within the PM group, as evidenced by a p-value of less than 0. 0001. The TUNEL analysis revealed a significantly higher count of TUNEL-positive cells in the PM group. Significantly, DQ counteracted the decline in MMP caused by PM (p<0.05, Figure 6 A,B).

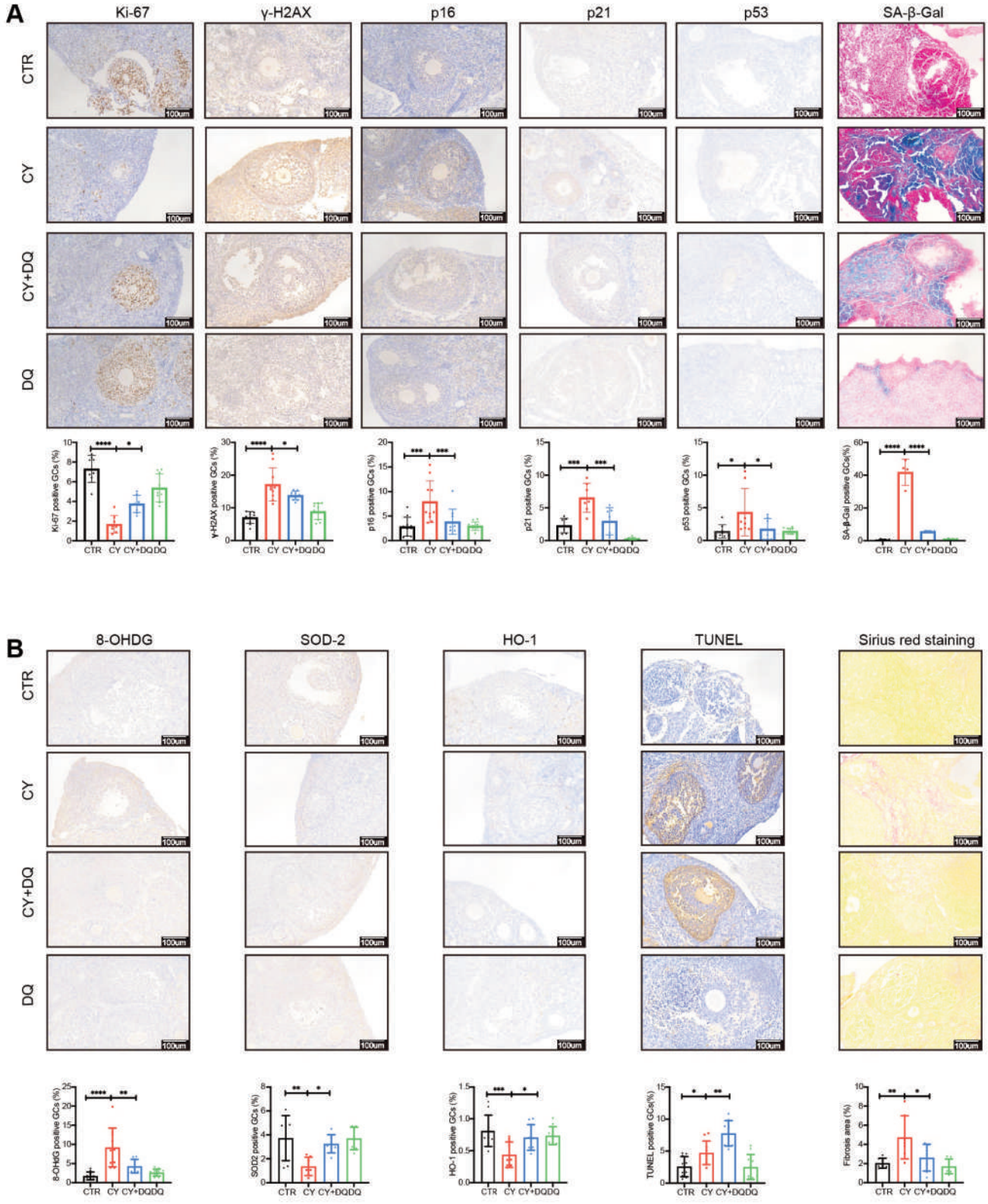

Figure 3. DQ alleviates cellular senescence, DNA damage, fibrosis, and regulates cellular apoptosis in CY-induced POI mice (n=3). **A**) Representative images of Ki-67, p16, p21, p53, and γ-H2AX expression in murine ovaries obtained by IHC, and SA-β-gal staining images of murine ovarian sections. **B**) Representative images of IHC staining (8-OHdG, SOD2, and HO1), TUNEL staining, and Sirius Red-stained ovaries. All values were displayed as mean ±SD; scale bars: 100 μm. One-way ANOVA was used for statistical analysis; *p<0.05, **p<0.01, ***p 0.001; ****p<0.0001.

Furthermore, while DQ did not alter the basal apoptotic rate in healthy KGN cells (DQ group), it significantly increased the rate of apoptosis in PM-induced senescent KGN cells (PM+DQ group) (Figure 6 C,D), further supporting its selective senolytic activity.

Discussion

Chemotherapy is the prevalent therapeutic approach for managing malignancies, with CY being a commonly utilized medication in clinical practice. CY is a chemotherapeutic agent that is commonly used in cancer treatment and has been subject to extensive research.[29] CY, as an alkylating agent, induces DNA double-strand breaks, leading to genomic damage and adverse effects on various organ systems, especially the ovaries. The toxicity of this substance is attributed to various underlying mechanisms, such as oxidative stress, inflammation, and apoptosis.[30] At present, there are no recognized pharmaceutical treatments available for CY-induced ovarian damage. Cellular senescence is defined by an irreversible cessation of cell division. It is commonly acknowledged that the process of aging is closely linked to the accumulation of senescent cells within tissues.[31] Senescence is primarily driven by the SASP and DNA damage.[32] Recent investigations indicate that the senescence-inducing mechanism of CY is not specific to cancer cells; it also impacts non-malignant organs, resulting in off-target complications such as accelerated reproductive senescence and compromised fertility.[33,34] Recognizing cellular senescence as a crucial factor in chemotherapy-induced damage highlights its potential as a therapeutic target. Despite the increasing acknowledgment of its significance, the precise alterations in cellular senescence within regular ovarian tissue after CY treatment remain largely uncharted territory. Therefore, understanding the dynamics of cellular senescence in this scenario has major implications for comprehending the mechanisms behind chemotherapy-induced ovarian damage and could assist in developing innovative treat-

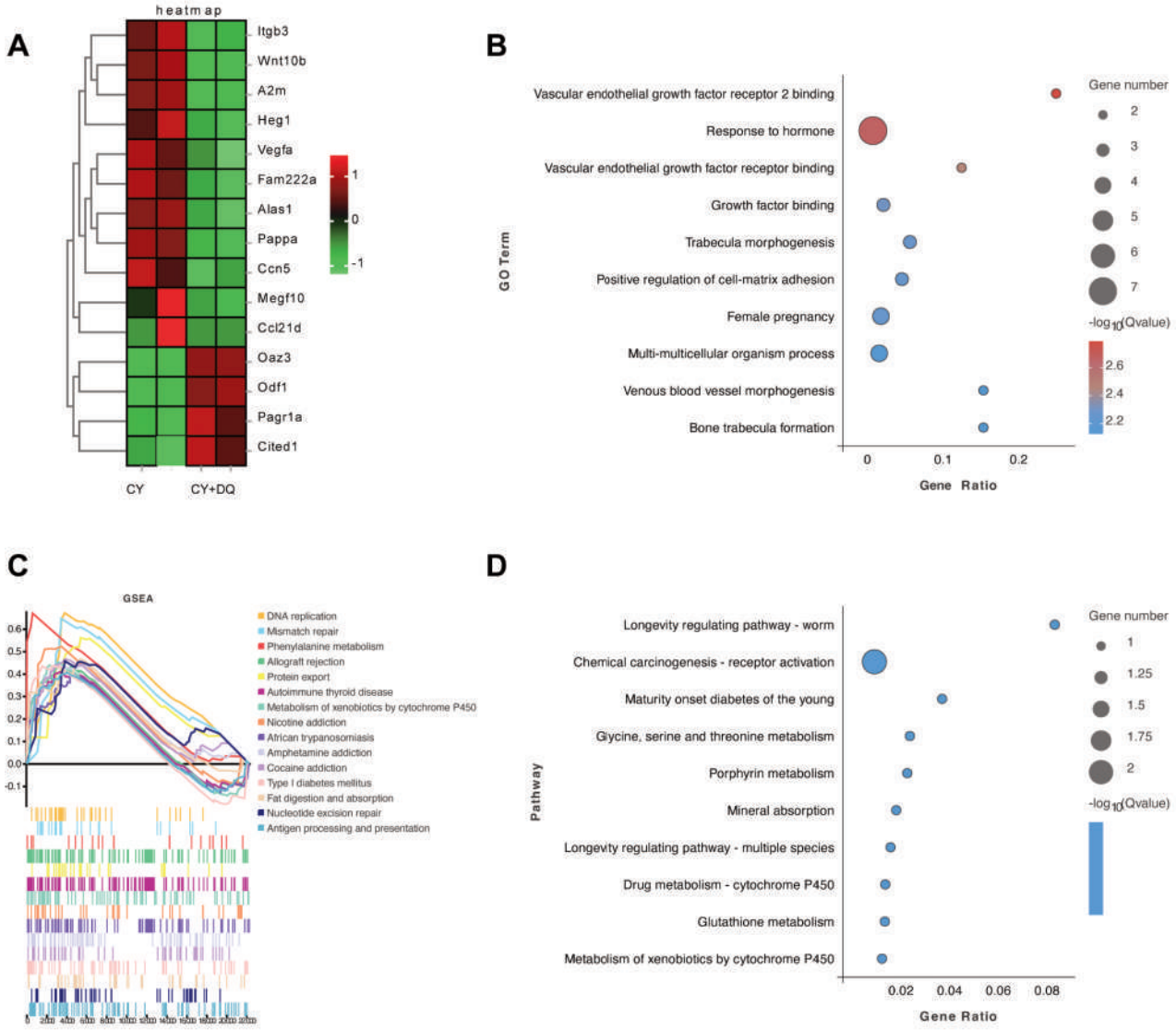

Figure 4. DQ regulates cell development in the CY-induced POI model mice. **A**) Heat map of DEGs in the ovaries treated with different medication regimens. **B-D**) GO, GSEA, and KEEG enrichment results according to transcriptional analysis (n=3).

ments to alleviate its negative consequences. This research sheds light on the impact of CY on the aging process of granulosa cells. In our study, we investigated the expression levels of p16, p21, and p53. In the CY-induced POI mouse model, granulosa cells of antral follicles were found to have elevated levels of γ-H2AX. SA-β-gal staining, a commonly employed indicator for senescent cells, identifies the lysosomal enzyme activity typical of cellular senescence. This phenomenon can be observed in senescent cells and tissues.[31] SASP, a complex array of cytokines and chemokines, is involved in various biological processes. The secretion of growth factors by senescent cells acts as a characteristic marker and plays a role in the paracrine signaling network that regulates senescence-associated responses. Moreover, p53 plays a crucial role in governing senescence-associated pathways, encompassing the maintenance of genome integrity and the regulation of SASP components. In order to substantiate this hypothesis, we carried out cell-based experiments. The results showed that PM, which is an active metabolite of CY, increased the activity of SA-β-gal in human KGN cells. Furthermore, q-PCR analysis indicated that the expression of numerous shared SASP genes, such as *p53*, *γ-H2AX*, *CCL2*, *Il-6*, and *Il-8*, was significantly increased. This aligns with prior research suggesting that PM elevates the percentage of SA-β-gal-positive KGN cells.[35] Our investigation revealed significant alterations in biomarker levels, suggesting that cellular senescence

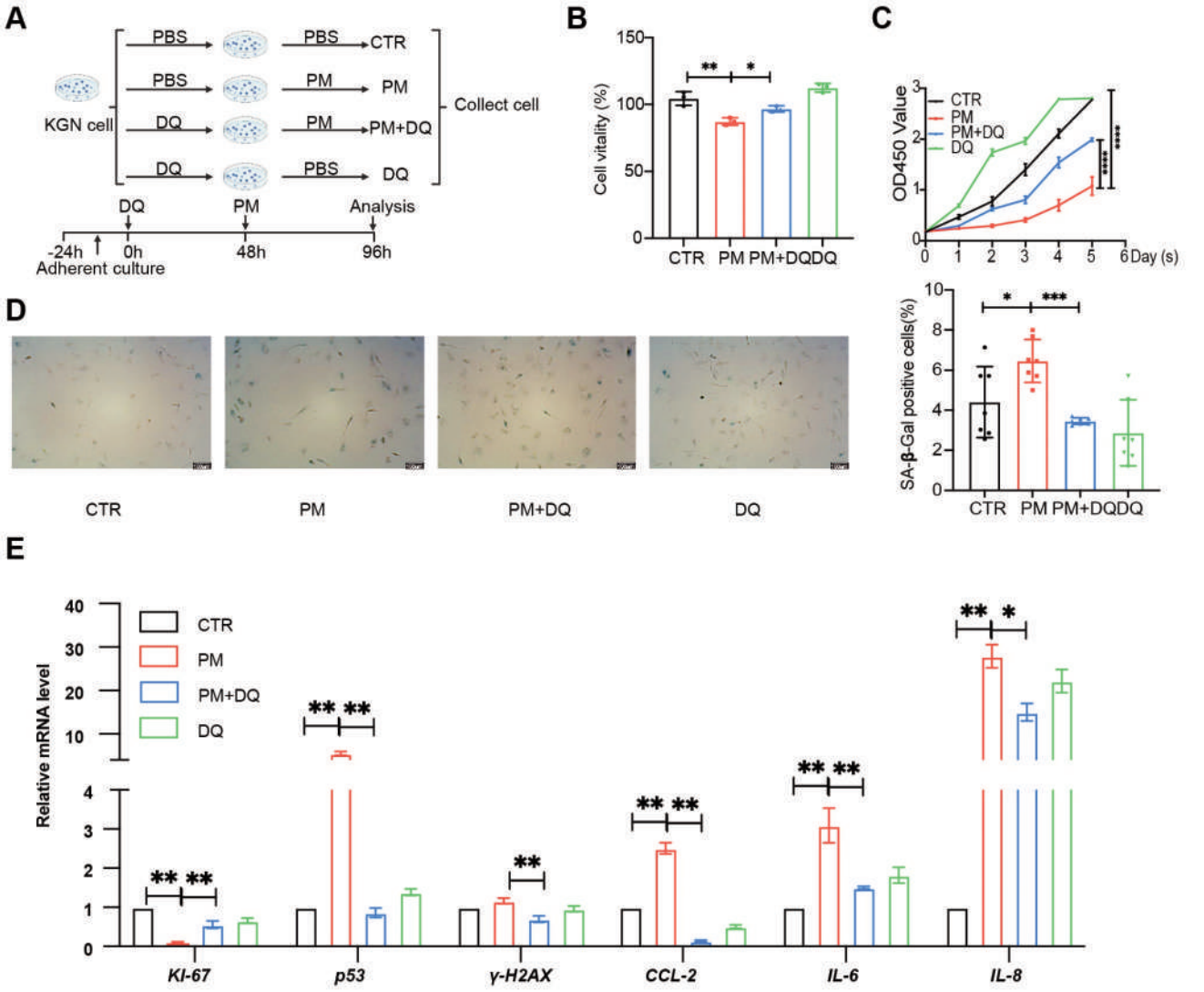

Figure 5. DQ reduced senescent granulosa cells and SASP caused by CY *in vitro*. **A**) Flowchart of KGN cells in vitro experiment. **B,C**) Cell viability and the proliferation rate of KGN cells in different groups. **D**) Light microscopic images of SA-β-gal-stained KGN cells and quantitative analysis of SA-β-gal-positive KGN cells (n=7); scale bars: 100 μm. **E**) Relative mRNA expression levels of genes involved in cellular senescence (n=3). All values were displayed as mean ±SD. One-way ANOVA was used for statistical analysis; **p*<0.05, ***p*<0.01, ****p*<0.001.

plays a crucial role in the CY-induced POI mouse model.

Therefore, we hypothesize that eliminating senescent cells could potentially partially restore ovarian function. In recent years, there has been extensive research on the anti-aging effects of D and Q, both individually and in combination, due to their potential benefits. Accumulated evidence suggests that the D and Q cocktail promotes the clearance of senescent cells, resulting in restored organ function across multiple conditions, such as metabolic disorders (type 2 diabetes), skeletal deterioration (osteoporosis), cardiovascular issues, and fibrotic or neurodegenerative diseases.[36-38] Early-stage clinical trials indicate that the Dasatinib and Quercetin cocktail effectively alleviates pathological manifestations in the lungs and kidneys of subjects with diabetic nephropathy and pulmonary fibrosis, while concurrently suppressing markers of biological aging.[39,40] It is important to highlight that while DQ intervention successfully alleviates cisplatin-mediated ovarian injury, previous studies indicate it confers no protective benefit regarding reproductive capacity or follicular reserve in doxorubicin-induced

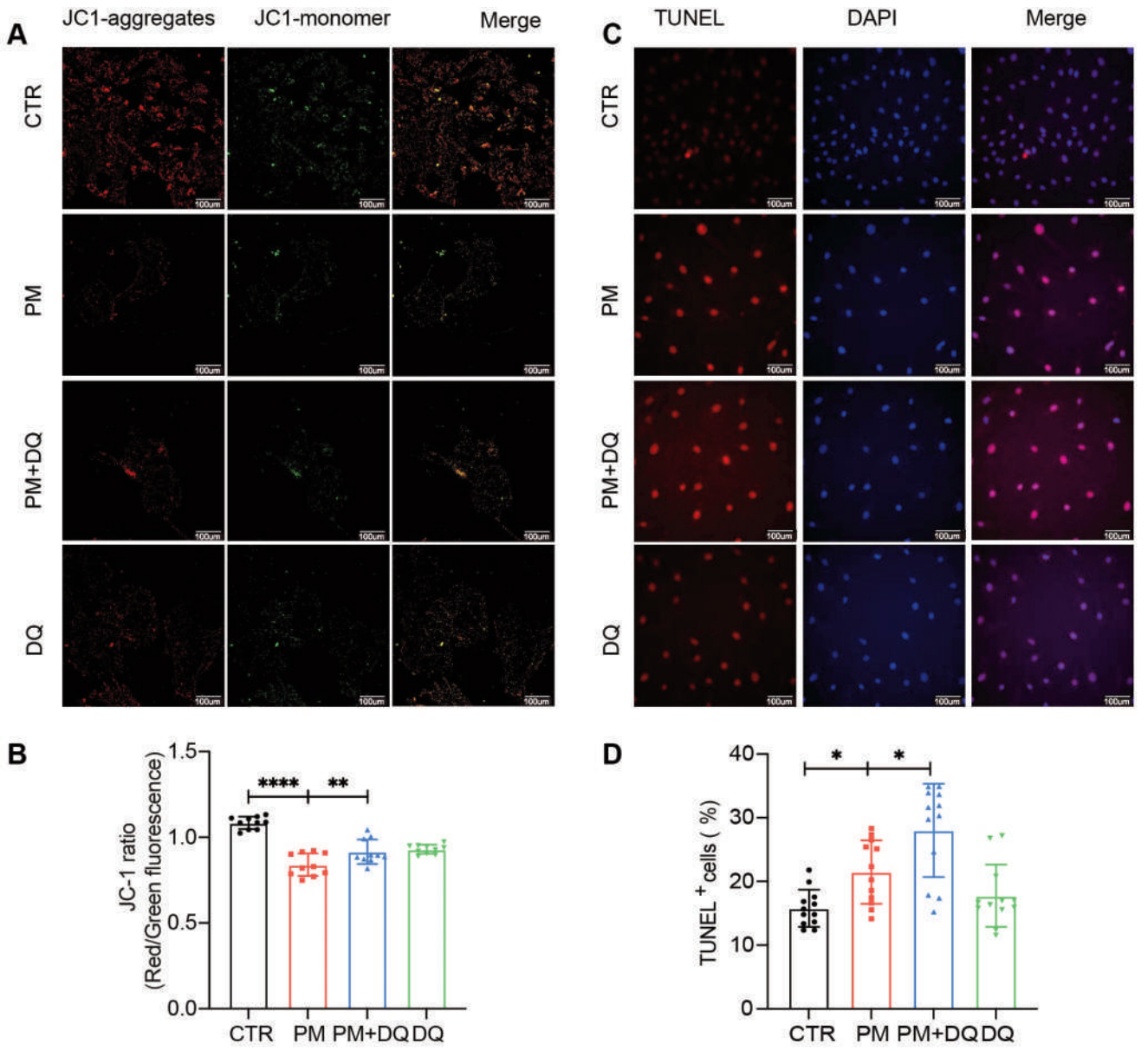

Figure 6. DQ regulates cellular MMP and apoptosis in PM-induced KGN cells. **A**) Representative JC-1 immunofluorescent staining. **B**) Quantitative analysis of the Red/Green JC-1 ratio; the n=10 represents the number of independent fields of view analyzed across 3 biological replicates. **C**) Representative TUNEL assay images. **D**) Ratio of apoptotic cells to total cells; the n=12 represents the number of independent fields of view analyzed across 3 biological replicates; scale bars: 100 μm. One-way ANOVA was used for statistical analysis; *p<0.05, **p<0.01, ****p<0.0001.

POI contexts.[14,41] Our recent investigation confirms the distinct ability of DQ to eliminate senescence and preserve ovarian function, aligning with prior research findings.[14,41] When conducting Q-PCR analysis on murine ovarian tissues and KGN cells, it was observed that the CY+DQ group exhibited a significant reduction in the secretion of inflammatory cytokines compared to the CY group. Notably, the CY+DQ group demonstrated a significant decrease in SA-β-gal staining, highlighting DQ's considerable senolytic capacity in ovarian tissues. Transcriptomic data derived from human preadipocytes suggest that senescent cells mirror cancer cells in their ability to bypass programmed cell death, a trait driven by the overexpression of specific pro-survival pathways.[42,43] Prior research has demonstrated that the co-administration of D and Q triggers programmed cell death in particular senescent cell types and mitigates senescence-associated characteristics in mice.[21] In comparison to mice that received CY treatment alone, the ratio of TUNEL-positive granulosa cells in the ovary of CY+DQ animals was notably increased. It suggests that DQ could potentially improve ovarian function by causing the demise of senescent granulosa cells. In order to delve deeper into the molecular processes underlying DQ, a transcriptome analysis was carried out. The ovaries of the CY+DQ group showed a notable increase in genes related to extraembryonic developmental regulation. The CY+DQ group showed reduced expression of genes responsible for triggering senescence, along with those associated with immunological and inflammatory reactions. Analysis using GO and KEGG revealed that DQ treatment positively regulated biological processes associated with female pregnancy, multicellular organism processes, and longevity pathways. Collectively, these findings substantiate that DQ exerts a multifaceted protective effect: beyond merely suppressing cellular senescence, it modulates diverse biological pathways to safeguard ovarian viability following chemotherapy.

Transcriptomic analysis revealed how DQ rescues the ovarian microenvironment through key DEGs. Specifically, DQ downregulated Itgb3 (a key driver of senescence and SASP) and Ccl21d (a pro-inflammatory chemokine). Suppressing Itgb3 aligns with the clearance of senescent granulosa cells and reduced stromal fibrosis, while reducing Ccl21d dampens local inflammation, protecting surviving follicles from atresia. Conversely, DQ upregulated Pagr1a, a gene linked to developmental regulation, suggesting a restored capacity for healthy folliculogenesis. Together, these genetic changes demonstrate that DQ not only clears senescent cells but actively reprograms the ovarian niche from a fibrotic, inflammatory state back to a healthy, pro-developmental environment.

clearing senescent cells, DQ's ability to rescue the ovarian reserve and restore endocrine function holds profound clinical significance for AYA cancer survivors. Chemotherapy-induced POI not only causes infertility but also precipitates premature menopause, exposing patients to estrogen deprivation and severe comorbidities like osteoporosis and cardiovascular disease. By preserving the follicle pool and restoring physiological estradiol and AMH levels, senolytic therapy offers a vital dual benefit. First, it maintains systemic endocrine homeostasis, protecting patients from the long-term consequences of premature menopause. Second, it preserves the functional ovarian reserve for future family building through natural conception or assisted reproductive technologies. Thus, targeting cellular senescence is a highly translatable strategy to protect both the reproductive and systemic health of female cancer patients. Translating DQ therapy into clinical practice requires establishing age-appropriate dosing for young cancer patients to avoid off-target toxicities. Importantly, to prevent exacerbating systemic toxicity or interfering with CY's antineoplastic efficacy, senolytics should not be administered concurrently. Instead, a sequential 'hit-and-run' strategy deployed after chemotherapy cycles offers the safest clinical approach. Future studies must optimize the pharmacokinetic compatibility of DQ with existing oncological protocols for fertility preservation.

Several limitations in this study warrant consideration. First, the absence of mating trials limits our ability to assess live birth rates and offspring health. Because senolytics cannot repair CY-induced genomic damage within the germline, future studies must rigorously evaluate the genetic fidelity of rescued oocytes to rule out transmitted defects. Second, while our investigation centered on granulosa cells, DQ likely exerts broader protective effects across the ovarian niche such as clearing senescent stromal fibroblasts, providing paracrine protection to oocytes via SASP reduction, and modulating immune cells. Future single-cell RNA sequencing and dual-labeling assays (e.g., p16/TUNEL) are necessary to definitively map these multi-cellular dynamics and confirm target specificity. Third, our short-term murine model necessitates further dose-optimization studies to establish long-term safety profiles and clinical eligibility guidelines for human translation. Despite these limitations, our findings robustly demonstrate that short-term DQ therapy effectively clears CY-induced senescent cells, preserves the follicle pool, and restores ovarian function, highlighting senolytics as a highly promising strategy to mitigate chemotherapy-induced reproductive toxicity.

References

1. Bender JL, Puri N, Salih S, D'Agostino NM, Tsimicalis A, Howard AF, et al. Peer support needs and preferences for digital peer navigation among adolescent and young adults with cancer: a Canadian cross-sectional survey. Curr Oncol 2022;29:1163-75.
2. Rodriguez-Wallberg KA, Jiang Y, Lekberg T, Nilsson HP. The late effects of cancer treatment on female fertility and the current status of fertility preservation-A narrative review. Life (Basel) 2023;13:1195.
3. Tanner S, Engstrom T, Lee WR, Forbes C, Walker R, Bradford N, et al. Mental health patient-reported outcomes among adolescents and young adult cancer survivors: A systematic review. Cancer Med 2023;12:18381-93.
4. Dai F, Wang R, Deng Z, Yang D, Wang L, Wu M, et al. Comparison of the different animal modeling and therapy methods of premature ovarian failure in animal model. Stem Cell Res Ther 2023;14:135.
5. Overbeek A, van den Berg MH, van Leeuwen FE, Kaspers GJL, Lambalk CB, van Dulmen-den Broeder E. Chemotherapy-related late adverse effects on ovarian function in female survivors of childhood and young adult cancer: A systematic review. Cancer Treat Rev 2017;53:10-24.
6. Prasanna PG, Citrin DE, Hildesheim J, Ahmed MM, Venkatachalam S, Riscuta G, et al. Therapy-induced senescence: opportunities to improve anticancer therapy. J Natl Cancer Inst 2021;113:1285-98.
7. Ai G, Meng M, Guo J, Li C, Zhu J, Liu L, et al. Adipose-derived stem cells promote the repair of chemotherapy-induced premature ovarian failure by inhibiting granulosa cells apoptosis and senescence. Stem Cell Res Ther 2023;14:75.
8. Dolmans M, Manavella DD. Recent advances in fertility preservation. J Obstet Gynaecol Re 2019;45:266-79.
9. Harada M, Osuga Y. Fertility preservation for female cancer

patients. Int J Clin Oncol 2019;24:28-33.
10. Yang Y, Tang X, Yao T, Zhang Y, Zhong Y, Wu S, et al. Metformin protects ovarian granulosa cells in chemotherapy-induced premature ovarian failure mice through AMPK/PPAR-gamma/SIRT1 pathway. Sci Rep 2024;14:1447.
11. Marcozzi S, Rossi V, Salvatore G, Di Rella F, De Felici M, Klinger FG. Distinct effects of epirubicin, cisplatin and cyclophosphamide on ovarian somatic cells of prepuberal ovaries. Aging (Albany NY) 2019;11:10532-56.
12. Xu Z, Takahashi N, Harada M, Kunitomi C, Kusamoto A, Koike H, et al. The role of cellular senescence in cyclophosphamide-induced primary ovarian insufficiency. Int J Mol Sci 2023;24:17193.
13. Ogrodnik M, Evans SA, Fielder E, Victorelli S, Kruger P, Salmonowicz H, et al. Whole-body senescent cell clearance alleviates age-related brain inflammation and cognitive impairment in mice. Aging Cell 2021;20:e13296.
14. Du D, Tang X, Li Y, Gao Y, Chen R, Chen Q, et al. Senotherapy protects against cisplatin-induced ovarian injury by removing senescent cells and alleviating DNA damage. Oxid Med Cell Longev 2022;2022:9144644.
15. Cora MC, Kooistra L, Travlos G. Vaginal cytology of the laboratory rat and mouse: review and criteria for the staging of the estrous cycle using stained vaginal smears. Toxicol Pathol 2015;43:776-93.
16. Bernstein LR, Mackenzie ACL, Kraemer DC, Morley JE, Farr S, Chaffin CL, et al. Shortened estrous cycle length, increased FSH levels, FSH variance, oocyte spindle aberrations, and early declining fertility in aging senescence-accelerated mouse prone-8 (SAMP8) mice: concomitant characteristics of human midlife female reproductive aging. Endocrinology 2014;155:2287-300.
17. Myers M, Britt KL, Wreford NGM, Ebling FJP, Kerr JB. Methods for quantifying follicular numbers within the mouse ovary. Reproduction 2004;127:569-80.
18. Zhang Q, Huang Y, Sun J, Gu T, Shao X, Lai D. Immunomodulatory effect of human amniotic epithelial cells on restoration of ovarian function in mice with autoimmune ovarian disease. Acta Bioch Bioph Sin (Shanghai) 2019;51:845-55.
19. Sola M, Magrin C, Pedrioli G, Pinton S, Salvade A, Papin S, et al. Tau affects P53 function and cell fate during the DNA damage response. Commun Biol 2020;3:245.
20. Wang Z, Han N, Zhao K, Li Y, Chi Y, Wang B. Protective effects of pyrroloquinoline quinine against oxidative stress-induced cellular senescence and inflammation in human renal tubular epithelial cells via Keap1/Nrf2 signaling pathway. Int Immunopharmacol 2019;72:445-53.
21. Zhu Y, Tchkonia T, Pirtskhalava T, Gower AC, Ding H, Giorgadze N, et al. The Achilles' heel of senescent cells: from transcriptome to senolytic drugs. Aging Cell 2015;14:644-58.
22. Ruggiero AD, Vemuri R, Blawas M, Long M, DeStephanis D, Williams AG, et al. Long-term dasatinib plus quercetin effects on aging outcomes and inflammation in nonhuman primates: implications for senolytic clinical trial design. Geroscience 2023;45:2785-803.
23. Chen Y, Wen J, Li Q, Peng D, Liao C, Ma X, et al. RAB27B-regulated exosomes mediate LSC maintenance via resistance to senescence and crosstalk with the microenvironment. Leukemia 2024;38:266-80.
24. Misu M, Ouji Y, Kawai N, Nishimura F, Nakamura-Uchiyama F, Yoshikawa M. Effects of Wnt-10b on proliferation and differentiation of murine melanoma cells. Biochem Bioph Res Commun 2015;463:618-23.
25. St Sauver JL, Weston SA, Atkinson EJ, Mc Gree ME, Mielke MM, White TA, et al. Biomarkers of cellular senescence and risk of death in humans. Aging Cell 2023;22:e14006.
26. Bi S, Jiang X, Ji Q, Wang Z, Ren J, Wang S, et al. The sirtuin-associated human senescence program converges on the activation of placenta-specific gene PAPPA. Dev Cell 2024;59:991-1009.
27. Ma J, Liu M, Wang Y, Xin C, Zhang H, Chen S, et al. Quantitative proteomics analysis of young and elderly skin with DIA mass spectrometry reveals new skin aging-related proteins. Aging (Albany NY) 2020;12:13529-54.
28. Cao W, Du YC, Li Y, Wu XJ, Zhang AZ. [Effect of cigarette smoke exposure on the expression of CCR7 and levels of Th1/Th2 cytokines in asthmatic rats].[Article in Chinese]. Zhonghua Yi Xue Za Zhi 2018;98:2264-8.
29. Codacci-Pisanelli G, Del Pup L, Del Grande M, Peccatori FA. Mechanisms of chemotherapy-induced ovarian damage in breast cancer patients. Crit Rev Oncol Hemat 2017;113:90-6.
30. Elkady MA, Shalaby S, Fathi F, El-Mandouh S. Effects of quercetin and rosuvastatin each alone or in combination on cyclophosphamide-induced premature ovarian failure in female albino mice. Hum Exp Toxicol 2019;38:1283-95.
31. Hernandez-Segura A, Nehme J, Demaria M. Hallmarks of cellular senescence. Trends Cell Biol 2018;28:436-53.
32. Hernandez-Segura A, de Jong TV, Melov S, Guryev V, Campisi J, Demaria M. Unmasking transcriptional heterogeneity in senescent cells. Curr Biol 2017;27:2652-60.
33. Marcozzi S, Rossi V, Salvatore G, Di Rella F, De Felici M, Klinger FG. Distinct effects of epirubicin, cisplatin and cyclophosphamide on ovarian somatic cells of prepuberal ovaries. Aging (Albany NY) 2019;11:10532-56.
34. Athira VR, Shivanandappa T, Yajurvedi HN. Cyclophosphamide, a cancer chemotherapy drug-induced early onset of reproductive senescence and alterations in reproductive performance and their prevention in mice. Drug Chem Toxicol 2022;45:760-6.
35. Chen S, Wang Y, Liao L, Meng L, Li J, Shi C, et al. Similar repair effects of human placenta, bone marrow mesenchymal stem cells, and their exosomes for damaged SVOG ovarian granulosa cells. Stem Cells Int 2020;2020:8861557.
36. Tchkonia T, Kirkland JL. Aging, cell senescence, and chronic disease: emerging therapeutic strategies. JAMA 2018;320:1319-20.
37. Gonzales MM, Garbarino VR, Kautz TF, Palavicini JP, Lopez-Cruzan M, Dehkordi SK, et al. Senolytic therapy in mild Alzheimer's disease: a phase 1 feasibility trial. Nat Med 2023;29:2481-8.
38. Wang Y, Che L, Chen X, He Z, Song D, Yuan Y, et al. Repurpose dasatinib and quercetin: Targeting senescent cells ameliorates postmenopausal osteoporosis and rejuvenates bone regeneration. Bioact Mater 2023;25:13-28.
39. Hickson LJ, Langhi Prata LGP, Bobart SA, Evans TK, Giorgadze N, Hashmi SK, et al. Senolytics decrease senescent cells in humans: Preliminary report from a clinical trial of Dasatinib plus Quercetin in individuals with diabetic kidney disease. Ebiomedicine 2019;47:446-56.
40. Justice JN, Nambiar AM, Tchkonia T, LeBrasseur NK, Pascual R, Hashmi SK, et al. Senolytics in idiopathic pulmonary fibrosis: Results from a first-in-human, open-label, pilot study. Ebiomedicine 2019;40:554-63.
41. Gao Y, Wu T, Tang X, Wen J, Zhang Y, Zhang J, et al. Increased cellular senescence in doxorubicin-induced murine

ovarian injury: effect of senolytics. Geroscience 2023;45:1775-90.
42. Zhu Y, Tchkonia T, Fuhrmann-Stroissnigg H, Dai HM, Ling YY, Stout MB, et al. Identification of a novel senolytic agent, navitoclax, targeting the Bcl-2 family of anti-apoptotic factors. Aging Cell 2016;15:428-35.
43. Yin J, Chang H, Li R, Leung PC. Recent progress in the treatment of women with diminished ovarian reserve. Gynecol Obstet Clin Med 2021;1:186-9.

Received: 30 January 2026. Accepted: 25 March 2026.

Licensee PAGEPress, Italy
European Journal of Histochemistry 2026; 70:4537
doi:10.4081/ejh.2026.4537